Splanchnic tissues undergo hypoxic stress during whole body hyperthermia

DAVID M. HALL,[1,2] KIRK R. BAUMGARDNER,[3] TERRY D. OBERLEY,[4] AND CARL V. GISOLFI[1]
[1]*Department of Exercise Science and* [2]*The Free Radical Research Institute, The University of Iowa, Iowa City, Iowa 52242;* [3]*Department of Cariology, Restorative Sciences, and Endodontics, The University of Michigan, Ann Arbor, Michigan 48109-1078; and* [4]*Department of Pathology, William H. Middleton Memorial Veterans Affairs Hospital, Madison, Wisconsin 53705*

Hall, David M., Kirk R. Baumgardner, Terry D. Oberley, and Carl V. Gisolfi. Splanchnic tissues undergo hypoxic stress during whole body hyperthermia. *Am. J. Physiol.* 276 (*Gastrointest. Liver Physiol.* 39): G1195–G1203, 1999.— Exposure of conscious animals to environmental heat stress increases portal venous radical content. The nature of the observed heat stress-inducible radical molecules suggests that hyperthermia produces cellular hypoxic stress in liver and intestine. To investigate this hypothesis, conscious rats bearing in-dwelling portal venous and femoral artery catheters were exposed to normothermic or hyperthermic conditions. Blood gas levels were monitored during heat stress and for 24 h following heat exposure. Hyperthermia significantly increased arterial O_2 saturation, splanchnic arterial-venous O_2 difference, and venous P_{CO_2}, while decreasing venous O_2 saturation and venous pH. One hour after heat exposure, liver glycogen levels were decreased ~20%. Two hours after heat exposure, the splanchnic arterial-venous O_2 difference remained elevated in heat-stressed animals despite normal T_c. A second group of rats was exposed to similar conditions while receiving intra-arterial injections of the hypoxic cell marker [3H]misonidazole. Liver and intestine were biopsied, and [3H]misonidazole content was quantified. Heat stress increased tissue [3H]misonidazole retention 80% in the liver and 29% in the small intestine. Cellular [3H]misonidazole levels were significantly elevated in intestinal epithelial cells and liver zone 2 and 3 hepatocytes and Kupffer cells. This effect was most prominent in the proximal small intestine and small liver lobi. These data provide evidence that hyperthermia produces cellular hypoxia and metabolic stress in splanchnic tissues and suggest that cellular metabolic stress may contribute to radical generation during heat stress.

heat stress; free radical; reactive oxygen species; oxidative stress; hypoxia

WHOLE BODY HYPERTHERMIA elevates total oxygen consumption, stimulates cellular metabolism (28), and progressively decreases blood flow to splanchnic viscera (stomach, spleen, liver, and intestine) (27). At colonic temperatures (T_c) >39°C, hyperthermia can also produce lesions in the heart, lungs, liver, kidneys, and gastrointestinal tract (16, 42). In particular, we have observed that the intestine and liver appear to be critical target tissues for heat stress-related injury (21, 41). We have also observed that the intestine and liver express high levels of primary antioxidant enzymes following heat challenge (D. M. Hall, K. C. Kregel, L. W. Oberley, P. L. Moseley, C. V. Gisolfi, and T. D. Oberley, unpublished observations), suggesting that heat stress stimulates reactive oxygen species (ROS) production in both organs. On the basis of these results and similar data from other groups (29, 31, 35, 40, 43–46), we have speculated that the combined effects of hyperthermia-induced ischemia and cellular metabolic stress promote cellular oxidative stress, which in turn may be involved in the pathogenesis of heat toxicity.

In support of this tenet, we recently reported that exposure of conscious animals to environmental heat stress progressively elevates splanchnic vascular concentrations of the radicals ceruloplasmin, semiquinone, and hemoglobin-nitric oxide (Hb-NO·) (20). A common link between these radical species is that production of all three can be stimulated by cellular hypoxia. Quantitation of vascular Hb-NO· levels has been used extensively as an index of alterations in ·NO production. The semiquinone radical is a marker of advanced respiratory chain reduction, a condition that can evolve when molecular oxygen is the rate-limiting substrate in oxidative phosphorylation. Ceruloplasmin is an acute phase protein released by the liver under conditions of inflammation or local hypoxia, both of which can rapidly stimulate ·NO and semiquinone radical generation. On the basis of these data and reports from the literature establishing that both the liver and intestine can develop oxygenation gradients during periods of low blood flow (18, 19, 26, 34, 36), we hypothesized that the intestine and liver may be subject to hypoxic stress during whole body heat stress.

With the use of ex vivo assessment of splanchnic blood gas levels with ramped elevation in T_c and the hypoxic cell marker misonidazole as a probe to identify hypoxic cells, the aim of the present study was to determine if heat stress produces cellular hypoxia in liver and intestine. Our results demonstrate that hyperthermia increases intestinal oxygen extraction, elevates intestinal metabolic acid production, and produces significant cellular hypoxia in the small intestine and liver. Hypoxia is prominent in regions of the intestine and liver that are sensitive to heat stress-related injury; therefore, these results suggest that cellular hypoxia and cellular metabolic stress may contribute to radical generation and oxidant-mediated injury during severe hyperthermia.

METHODS

Misonidazole

Misonidazole, 1-(2-hydroxy-3-methoxypropyl)-2-nitro-1H-imidazole (see Ref. 2), is a member of the bioreductive, 2-nitroimidazole family. Misonidazole has been used in experimental cancer therapy because of its ability to covalently bind to hypoxic cells, thereby sensitizing them to the free radical effects of ionizing radiation. Previous work establishes that misonidazole is selectively retained by hypoxic cells in tissue culture systems (38, 39, 51), intact animals (2, 3, 8, 9, 23, 30, 38), and humans (50).

The mechanism of cellular misonidazole retention involves activation through bioreduction of its nitro group, generating a radical anion intermediate (see Ref. 2). In the presence of molecular oxygen, this radical can be oxidized back to its parent compound through an electron transfer reaction with molecular oxygen. A futile redox cycle is established, yielding superoxide anion (O_2^-) as a by-product, with little net nitro reduction taking place (14). Decreasing oxygen tension within the cell favors four-electron reduction of misonidazole, culminating in generation of a highly reactive hydroxylamine that covalently binds to cellular RNA and proteins at the site of reduction (51). The bound hydroxylamine contains the entire skeleton of the original misonidazole compound and does not reflect binding of molecular fragments, which may be produced during metabolism; therefore, a radioactive label attached to misonidazole is retained as a marker only in the cell where bioreduction takes place (14, 39).

A method for radioactively labeling hypoxic cells with tritiated misonidazole ([3H]misonidazole) was first described by Chapman et al. (7). This technique has been used extensively to label hypoxic cells in tumors (7, 30, 50) and in normal tissues during inflammation, experimental ischemia, hypoxemia, and hypobaric hypoxia (2, 3, 8, 9, 30, 32, 38).

Procedures

Blood gas experiments. SURGICAL PREPARATION. Thirty-two male Sprague-Dawley rats (Harlan Sprague-Dawley, Indianapolis, IN) weighing 320–350 g served as subjects in these experiments. Rats were anesthetized with pentobarbital sodium (Nembutal, 50 mg/kg ip). A right inguinal incision was made, and a catheter (PE-50) filled with heparanized saline (100 U/ml) was placed in the femoral artery. A midline laparotomy was performed, the portal vein was isolated, and a second catheter (Silastic tubing over PE-10, Clay Adams, Parsippany, NJ) filled with heparinized saline was placed in a portal tributary vessel ∼5 mm from the liver. To avoid portal blood flow occlusion, the catheter was placed only in the tributary vessel and not in the portal vein itself. Catheter placement was confirmed at the end of each experiment.

Distal ends of both catheters were tunneled subcutaneously to the dorsal neck, exposed through an incision between the scapulae, and capped with stainless steel stylettes. Incisions were closed, and animals were allowed to recover for 3 days. During recovery, rats were maintained on a 12:12-h light-dark cycle at 22–24°C and received standard rat chow and water ad libitum. Animals were handled daily and were familiarized with colonic thermocouple probes and blood collection procedures. Venous blood samples (200 µl) were collected daily between 1300 and 1700 for complete blood count (CBC) with cell differential analyses. Animals with elevated white counts ($n = 2$), compared with CBCs determined the day of surgery, or overt signs of infection were not used in experiments.

PROTOCOL. Experiments were performed between 1300 and 1700. Euthermic sham-heated control and heat-stressed experimental rats were weight matched and fitted with rectal thermocouple probes (36-gauge copper-constantan wire in PE-100 tubing) inserted 6–7 cm beyond the anal sphincter. Experimental rats ($n = 16$) were heated in an environmental chamber (40°C dry bulb, 30% relative humidity) until T_c reached 41.5°C, then removed from the heat and allowed to cool passively at 22–24°C. Arterial and venous blood samples (250 µl) were collected in arterial blood gas syringes at T_c measurements of 37 (immediately before heating), 39, 40, 41, and 41.5°C and 1, 2, and 24 h after heat exposure and delivered to a Nova Biostat 3 blood gas analyzer (Nova Biomedical) for direct measurement of pH, P_{CO_2}, and P_{O_2}. From these data, percent O_2 saturation and arterial-venous O_2 difference were calculated. To minimize the effects of repeated blood sampling, rats received 1 ml of blood drawn from a littermate donor rat following sample collection at 39 and 41°C and 1 h after heat exposure. Euthermic sham-heated control rats ($n = 16$) were handled as heat-stressed rats except that they were maintained at 22–24°C. Blood samples were collected simultaneously from heat-exposed and sham-heated animals.

A cohort of animals ($n = 8$, 4 from each group) were killed 1 h after heat exposure by Nembutal overdose (80 mg/kg). Biopsies of liver lobus sinister and lobi caudatus dexter were rapidly excised and prepared for standard histological processing and glycogen staining. Hepatic glycogen content was contrasted between groups by comparing relative differences (%change) in the size of area staining positively for glycogen per 200 µm² tissue as defined by an eye-piece graticule. All slides were reviewed by the same evaluator who was blinded as to their origin.

[3H]misonidazole experiments. SURGICAL PREPARATION. In a second set of experiments, 14 rats were anesthetized as described in *Blood gas experiments* and fitted with indwelling left carotid artery catheters (PE-50, Clay Adams), advanced to the level of the ascending arch of the aorta. The distal end of each catheter was exposed at the dorsal neck, incisions were closed, and rats were allowed to recover from surgery for 3 days. Animals were handled daily and familiarized with colonic thermocouple probes. Blood was collected daily for CBC with differential. Animals with elevated white counts ($n = 1$) or overt signs of infection were not used in experiments.

PROTOCOL. Heat-exposed ($n = 8$) and sham-heated ($n = 6$) rats were weight matched, and heat-stressed animals were heated in an environmental chamber as described in *Blood gas experiments*. When T_c of 41.5°C was reached, [3H]misonidazole (Hoffmann-Laroche, Nutley, NJ) (20 mCi in isotonic saline suspension, 250 µl total volume) was delivered into the systemic circulations of both the hyperthermic rat and its sham-heated partner. Heat-stressed rats were removed from the heat, and both animals were maintained at 22–24°C for 24 h.

Misonidazole was labeled with tritium according to the method of Born and Smith (4). Unlabeled misonidazole was added to [3H]misonidazole according to the method of Baumgardner et al. (2, 3), so that each animal received 185 MBq of tritium at a total misonidazole dose of 75 mg/kg body wt.

Quantifying [3H]misonidazole retention. TISSUE HANDLING AND PREPARATION. Misonidazole reduction and the labeling of hypoxic cells occur within 1 h, and the drug is completely metabolized within 24 h (50). Twenty-four hours after heat stress was chosen as the optimum time point for collecting tissues to minimize including [3H]misonidazole present in

extracellular spaces as part of the hypoxic cell fraction, thereby overestimating the magnitude of tissue hypoxia (50).

Twenty-four hours after heat exposure, animals were killed by Nembutal overdose (80 mg/kg), followed by transcardial perfusion with a 10% neutral buffered Formalin solution. Biopsies of liver lobus sinister and lobi caudatus dexter and proximal, middle, and distal sections of the small intestine and colon were collected and processed for quantitation of [³H]misonidazole content using the method of Baumgardner et al. (2, 3).

Briefly, tissues were finely minced, placed in scintillation vials, and dried in a tissue oven at 105°C. Samples were then cooled under dry nitrogen gas, weighed, and rehydrated with 0.2 ml of double distilled water, followed by solubilization in 1 ml of Soluene 350 (Packard Instruments, Meriden, CT) for 12 h. Hionic fluor (15 ml; Packard Instruments) was added, and vials were placed in a Beckman LS 3801 liquid scintillation counter (Beckman Instruments, Fullerton, CA) where they were allowed to dark adapt for 72–96 h. Net sample counts per minute were corrected to dpm using a series of variably quenched tritium standards and the H number method (see Ref. 2). Sample activity was divided by its dry weight, with [³H]misonidazole retention expressed as dpm per milligram dry tissue.

To determine cellular [³H]misonidazole retention, sections of organ biopsies were fixed in a 10% neutral buffered Formalin solution for 48 h and processed through graded alcohols to paraffin. Sections 4-µm thick were placed on subbed slides, dewaxed and dipped in Kodak NTB2 autoradiographic nuclear track emulsion, and stored in light-tight boxes at 4°C. At 1, 2, 4, 8, 16, 32, 64, 128, and 256 days following NTB2 treatment, slides were removed from storage, developed using Kodak D19 developing solution and Kodak Fixer, stained with hematoxylin and eosin, and examined via light microscopy for adequate histological sectioning. [³H]misonidazole retention was quantified by counting grains overlying a minimum of 200 µm² tissue as defined by an eye-piece graticule. Background counts per unit area were obtained from the emulsion area immediately adjacent to the apical edge of each tissue section. Actual tissue grain counts were adjusted by subtracting background counts. All slides were reviewed by the same evaluator who was blinded as to their origin.

Calculations

Thermal stress was quantified by determining thermal load, a product of magnitude of T_c above 40.4°C and duration of hyperthermia (24). T_c was recorded at 1-min intervals, and thermal load (°C·min) was calculated as follows: Σ time interval (min) $\times$ [T_c (°C) above 40.4–40.4°C]. Heating rate (°C/min) was calculated as follows: [(peak T_c attained during heat exposure) − (normothermic baseline T_c)]/total heating time (min). Cooling rate (°C/min) was calculated as follows: (peak T_c)/(time to passively cool to T_c <40.4°C).

Statistics

Data represent mean values ± SD. Differences in blood gas values were analyzed by repeated-measures ANOVA. Significant differences were identified with the Scheffé's F test. Significance was set at $P \leq 0.05$. Groups for analyzing blood gas values were defined by treatment (hyperthermic vs. control) and by T_c (°C); therefore, both intragroup and intergroup comparisons were made with each degree rise in T_c of the heat-stressed group.

Differences in [³H]misonidazole concentrations between groups were compared using a two-sample t-test. Significant was set at $P \leq 0.05$. Groups were defined by treatment.

RESULTS

Comparisons of the thermal responses of heat-stressed rats in both studies show that there were no significant differences in heating rate, cooling rate, or magnitude of thermal stress between the two groups (Table 1). The thermal stress experienced by these animals was severe as rats spent 54 ± 5 and 56 ± 4 min, respectively, above T_c of 40.0°C, and peak T_c approached the estimated median lethal dose T_c for survival (42.5°C) (15). The relatively high cooling rates establish that both groups retained the ability to dissipate heat, and all animals survived 24 h after heat exposure.

Blood Gases

At T_c levels as low as 39–40°C, heat stress significantly increased portal venous P_{CO_2} and decreased venous P_{O_2}, pH, and percent venous O_2 saturation. With the exception of P_{CO_2}, these values remained significantly different from normothermic controls for 1–2 h after heat exposure (Table 2). Heat stress also increased femoral artery P_{O_2} and progressively decreased arterial P_{CO_2}. These values remained significantly different from controls for 1–2 h after heat exposure.

Coincident with changes in pH and partial pressure of the blood gases, the splanchnic arterial-venous O_2 difference was elevated more than 50% (58.9 ± 4.5 vs. 34.9 ± 1.6 mmHg) in the hyperthermic group and remained at a level significantly above that of normothermic controls for >2 h after heat stress (Table 2). T_c returned to normothermic levels in the experimental group within 55–65 min following cessation of heat exposure.

One hour after heat exposure, hepatic glycogen content was decreased in both lobus sinister and lobi caudatus dexter of all heat-stressed animals. In the control group, the percentage of cells staining positively for glycogen per 200 µm² was 96 ± 3%. Heat stress decreased the percentage of cells staining positively for glycogen by ~20% to 78 ± 7%. This effect was particularly evident in lobi caudatus dexter; here, the percentage of cells staining positively for glycogen fell to 72 ± 9%.

Table 1. *Thermal responses of rats during environmental heat stress (T_a of 40°C)*

Thermal Response	Blood Gas Experiments	[³H]Misonidazole Experiments
Baseline T_c, °C	37.4 ± 0.3	37.2 ± 0.4
Peak T_c, °C	41.7 ± 0.1	41.8 ± 0.2
Minutes above 40°C	54 ± 5.0	56 ± 4.0
Thermal load, °C min	39.6 ± 2.1	40.8 ± 3.3
Heating rate, °C/min	0.057 ± 0.004	0.059 ± 0.005
Cooling rate, °C/min	0.068 ± 0.005	0.071 ± 0.007

Values are means ± SD. Rats were exposed to environmental heat stress using a ramped protocol (T_a of 40°C) until colonic temperature (T_c) reached 41.5°C and then allowed to recover at 22–24°C. T_a, ambient temperature.

Table 2. Experimental and control blood gas parameters of portal venous and femoral artery blood collected from conscious rats during heat exposure

	37°C		39°C		40°C		41°C		41.5°C		1 h		2 h		24 h	
	Con	Hyp	Con	Hyp	Con	Hyp	Con	Hyp	Con	Hyp	Con	Hyp	Con	Hyp	Con	Hyp
a-vO$_2$ difference, mmHg	39.2±4.7	41.9±2.9	37.2±2.6	38.3±4.2	32.9±1.7	44.2±5.6‡	37.0±2.6	51.4±4.4‡	34.9±1.6	58.9±4.5‡	34.1±2.0	49.4±4.7‡	34.9±1.2	46.2±4.2‡	38.2±5.7	42.4±4.9
Po$_2$, mmHg																
PV	51.5±5.4	49.1±2.9	50.8±3.8	54.9±2.9*	53.3±3.6	48.5±4.4*	50.5±3.1	49.0±3.0	52.4±2.0	51.0±4.0	52.9±2.8	46.0±3.4†	52.2±2.6	46.5±2.9†	50.3±4.9	48.6±5.2
FA	89.2±4.0	91.0±3.2	88.0±2.2	93.2±1.5‡	86.2±3.6	92.7±4.2*	87.5±4.9	100.5±1.8‡	87.3±2.4	109.9±4.9‡	87.0±2.4	95.3±2.8‡	87.1±2.6	92.7±1.6‡	91.2±4.6	88.8±6.2
O$_2$ saturation, %																
PV	83.9±2.7	84.4±3.3	85.9±2.5	85.2±1.9	86.5±2.0	78.5±3.6‡	85.4±1.4	72.4±3.5‡	86.3±1.2	70.5±6.6‡	85.7±1.5	79.9±3.1‡	85.4±1.4	84.0±2.9	84.1±2.3	83.6±3.0
FA	96.9±0.9	97.6±0.2*	97.5±0.2	97.1±0.2†	97.3±0.4	96.9±0.2*	97.4±0.4	96.6±0.2‡	97.4±0.2	97.1±0.6	97.2±0.5	98.0±0.2‡	97.4±0.4	97.7±0.2*	97.2±0.4	97.5±0.3
Pco$_2$, mmHg																
PV	43.6±4.4	42.5±3.1	41.0±1.6	43.4±2.2*	41.8±3.5	42.4±2.7	41.3±2.3	45.9±4.8*	41.5±1.3	48.5±4.0†	41.9±1.3	40.6±3.0	41.3±2.3	42.1±2.1	43.8±5.4	42.1±3.9
FA	37.6±3.0	36.3±1.6	35.6±1.5	35.8±1.3	35.6±2.0	36.0±2.8	36.2±0.9	33.9±1.1‡	36.1±0.5	31.9±2.0‡	36.3±0.7	32.1±1.5‡	36.4±0.7	34.9±1.1*	37.2±3.3	36.8±2.4
pH																
PV	7.44±.03	7.42±.04	7.45±.01	7.43±.02*	7.44±.02	7.43±.02	7.45±.02	7.39±.02†	7.43±.01	7.35±.04‡	7.44±.01	7.41±.02*	7.45±.02	7.42±.02*	7.44±.02	7.43±.04
FA	7.47±.02	7.47±.01	7.48±.01	7.47±.01	7.47±.01	7.46±.02	7.48±.01	7.43±.01‡	7.48±.01	7.43±.01‡	7.47±.01	7.46±.02	7.47±.01	7.47±.02	7.47±.02	7.47±.01

Values are means ± SD. Rats were exposed to environmental heat stress using a ramped protocol (T$_a$ of 40.0°C) until T$_c$ reached 41.5°C then were allowed to recover at 22–24°C. Whole blood was collected at the indicated T$_c$ and analyzed for pH, Pco$_2$, and Po$_2$ concentrations. Data were compared between groups at each T$_c$. Con, control; Hyp, hyperthermic (heat exposed); PV, portal vein; FA, femoral artery; a-vO$_2$ difference, arterial-venous oxygen difference. * $P < 0.05$ vs. normothermic control; † $P < 0.001$ vs. normothermic control; ‡ $P < 0.0001$ vs. normothermic control.

[³H]Misonidazole Retention

Hyperthermia increased tissue tritium content 29% in the intestine (2,005 ± 54 vs. 1,550 ± 32 dpm/mg dry tissue, $P < 0.001$) and 80% in the liver (3,844 ± 90 vs. 2,117 ± 50 dpm/mg dry tissue, $P < 0.001$) (Fig. 1). Intestinal tritium retention in hyperthermic animals progressively decreased, moving from the duodenum to the proximal colon (Fig. 2). There were no differences in colonic [³H]misonidazole retention under either condition.

Autoradiographs of histological sections collected from the small intestine show that normothermic cellular retention of [³H]misonidazole was relatively homogeneous throughout the mucosa (Fig. 3). Neither serosal nor submucosal tissues retained notable concentrations of [³H]misonidazole under normothermic or hyperthermic conditions. However, heat stress markedly elevated label retention in villus epithelial cells (Fig. 3), with epithelial cell [³H]misonidazole concentration progressively increasing from the base of the villus to its tip. Epithelial cell [³H]misonidazole content plateaued in the upper third of each villus at a level twofold greater than normothermic cellular concentrations (Fig. 4). Mucosal epithelial cells were the only intestinal cell population with increased [³H]misonidazole retention following heat stress.

In hepatic tissues, there was a trend for elevated [³H]misonidazole retention under normothermic conditions in hepatocytes and Kupffer cells located between terminal branches of the hepatic artery or portal vein and corresponding hepatic venules (acinus zone 2 cells).
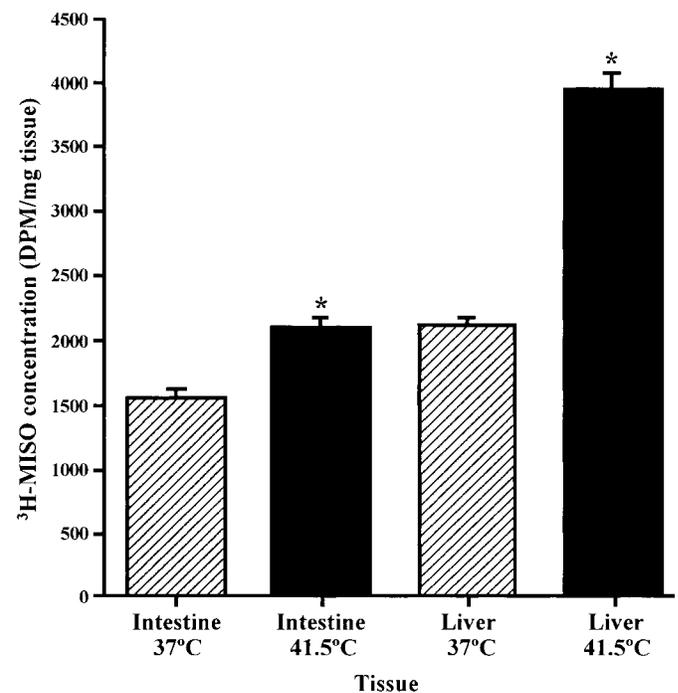

Fig. 1. Quantitation of tissue [³H]misonidazole (MISO) retention. Hyperthermia significantly increases intestinal and liver hypoxic label retention. Rats were exposed to environmental heat stress followed by intra-arterial injection of [³H]misonidazole as described in METHODS. Values represent means ± SD. *Significantly different from 37°C condition ($P < 0.001$).
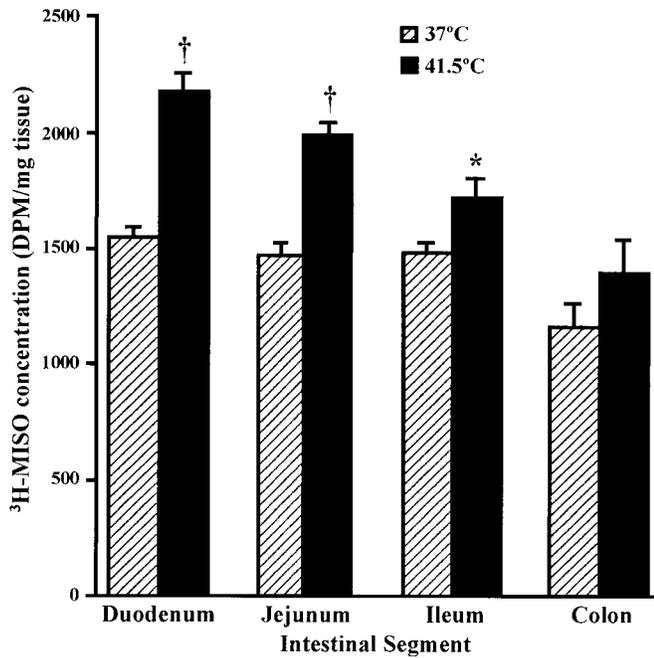
Fig. 2. Quantitation of segmental intestinal and colonic [³H]misonidazole retention. Hyperthermia increases [³H]misonidazole retention in small intestine but not in colon. Rats were exposed to environmental heat stress followed by intra-arterial injection of [³H]misonidazole as described in METHODS. Small intestine and colon were divided into 3 sections each (proximal, middle, and distal) and evaluated for [³H]misonidazole content. There were no differences between colon segments; therefore, data from these specimens were pooled. Values represent means ± SD. *Significantly different from 37°C condition ($P < 0.05$). †Significantly different from 37°C condition ($P < 0.001$).

This effect was more pronounced in lobi caudatus dexter, compared with larger liver lobules (Fig. 5). These data support previous reports that oxygen delivery can be heterogeneous in hepatic tissues, even under putative nonstress conditions (34).

Heat stress increased cellular [³H]misonidazole content more than 100% in zone 2 hepatocytes and ~50% in hepatocytes located adjacent to hepatic venules (zone 3 cells) (Fig. 5). Zone 2 and zone 3 Kupffer cells from hyperthermic animals retained [³H]misonidazole at concentrations too great to quantify (Fig. 6). Heat stress did not significantly alter hypoxic label retention in hepatocytes and Kupffer cells located adjacent to terminal branches of the hepatic artery or portal vein (zone 1 cells) (Figs. 5 and 6).

DISCUSSION

The purpose of this study was to test the hypothesis that heat stress produces cellular hypoxia and metabolic stress in liver and intestine. Our major findings support this idea, demonstrating that heat stress increases intestinal metabolic acid production, decreases hepatic glycogen content, and generates large regionalized zones of hypoxic cells in the intestinal mucosa and in the liver. Notably, cellular hypoxia occurred in regions of the intestine and liver that have high metabolic capacity and can develop arteriole-venule O_2 diffusional shunting (18, 19) or evolve gradients of tissue oxygenation (34) during periods of low blood flow. These are also tissues that are characteristically injured following thermal challenge (21, 41). On the basis of these results, we propose that cellular hypoxia contributes to hyperthermia-related injury in the liver and intestine. Mechanisms responsible for intestinal and hepatic injury are not clear, but previous reports
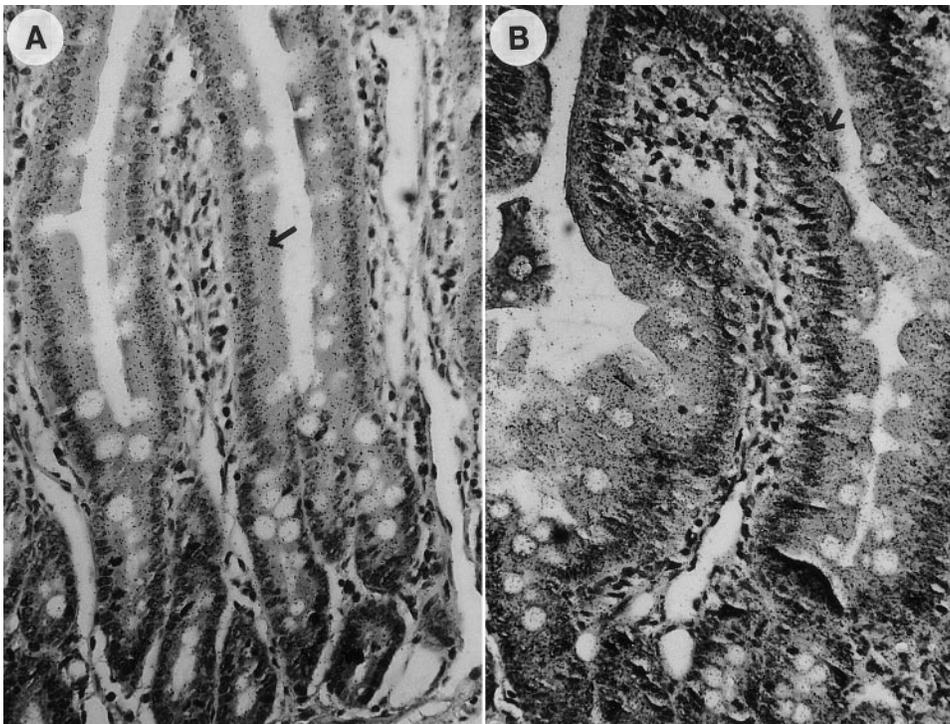

Fig. 3. Autoradiograph of histological intestinal sections collected from normothermic (A) and heat-stressed (B) rats, indicating localization of tritium label to hypoxic cells in the intestinal mucosa. Neither serosal nor submucosal tissues retained notable concentrations of [³H]misonidazole under normothermic or hyperthermic conditions. Hyperthermia markedly elevated label retention in villus epithelial cells. Arrows indicate epithelial cell containing the tritium label.
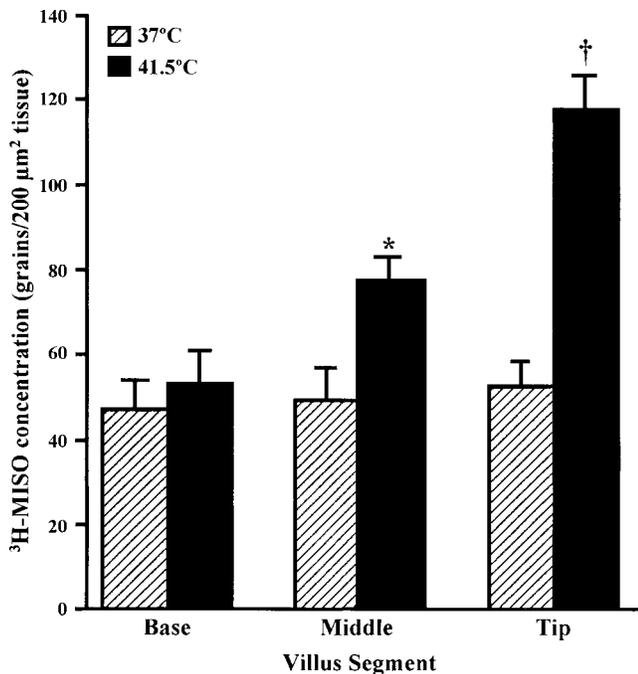
Fig. 4. Quantitation of small intestine epithelial cell [³H]misonidazole retention. Hyperthermia progressively elevates epithelial cell [³H]misonidazole retention from the base to tip of intestinal villi. Villi ($n = \sim 1{,}400$) were divided into 3 sections (base, middle, and tip) for quantification of epithelial cell [³H]misonidazole content. [³H]misonidazole retention was not different between villus sections under normothermic control conditions. Hyperthermia increased [³H]misonidazole retention $\sim 50\%$ in the middle third and $>100\%$ in the distal third of villi. Values represent means $\pm$ SD. *Significantly different from 37°C condition ($P < 0.05$). †Significantly different from 37°C condition ($P < 0.001$).

from our lab (20) and other groups (29, 35, 40, 43–46) strongly suggest that cellular oxidative stress may be elevated by thermal challenge. Moreover, it is known that heat stress can affect cellular energy-generating systems at several critical points, leading to ROS and reactive nitrogen species (RNS) production.

Blood Gases

In the present study, hyperthermia progressively increased splanchnic arterial-venous O_2 difference, increased portal venous P_{CO_2}, and decreased venous pH. These data suggest that heat stress increased oxygen consumption and stimulated metabolic acid production in intestinal tissues. We also observed that hepatic glycogen content was decreased in all heat-stressed rats. These results support our hypothesis that liver and intestine undergo metabolic stress during heat challenge. Mechanisms responsible for these effects are unclear, but the literature establishes that heat shock can uncouple oxidative phosphorylation, decreasing the ATP-to-O_2 ratio within the cell (28). Heat stress also stimulates activity of ATP-dependent membrane pumps (28), suggesting that hyperthermia can directly stimulate ATP use while simultaneously blunting ATP production. Under conditions in which the energy demand exceeds the ability to regenerate ATP, rapid depletion of cellular high-energy phosphate pools contribute to a

preferential use of glycolysis and progressive reduction of mitochondria electron transport centers. Increased cellular semiquinone radical production can evolve as a consequence of decreased electron flow through the complex IV cytochrome, promoting electron leak and univalent oxygen reduction from complexes I and III. There is considerable evidence that the resultant oxidative stress rapidly promotes disruption of the cellular cytoskeleton, short circuits membrane ion pumps (52), and leads to accumulation of intracellular ionized Ca^{2+} and Na^+ (11). Heat treatment of cells has been shown to produce similar results (28).

Exposing mitochondria to increased concentrations of ADP, Ca^{2+}, or Na^+ stimulates O_2^- and H_2O_2 production in a feedforward cycle that selectively impairs function of electron transport complex I, exacerbating ROS generation (11). Increased intracellular ionized Ca^{2+} can also stimulate ·NO production. We have previously observed that heat stress increases semiquinone radical and Hb-NO· production in vivo, suggesting that NO· production and ROS generation are stimulated by heat stress (20). Although the design of the present experiments did not include quantitation or characterization of splanchnic ROS production, data from the present study and results from our previous work support a scenario in which heat stress advances cellular oxidative stress through mechanisms similar to those previously elucidated for ischemia-reperfusion injury (33). However, rather than hinging on reintroduc-
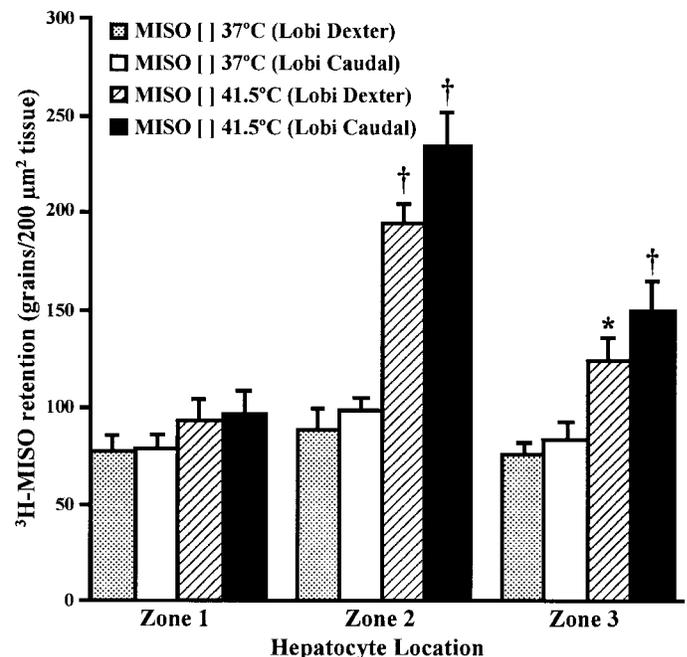

Fig. 5. Quantitation of hepatic [³H]misonidazole retention. Liver parenchymal cells were evaluated for [³H]misonidazole retention based on anatomic location. Zone 1 cells, around terminal hepatic arterioles or terminal portal venules; zone 2 cells, between artery or portal vein and corresponding hepatic vein; zone 3 cells, around the hepatic vein. Hyperthermia significantly increased [³H]misonidazole retention in zone 2 and zone 3 cells. This effect was significantly enhanced in lobi caudati compared with lobi dexter. Values represent means $\pm$ SD. *Significantly different from 37°C condition ($P < 0.05$). †Significantly different from 37°C condition ($P < 0.001$).
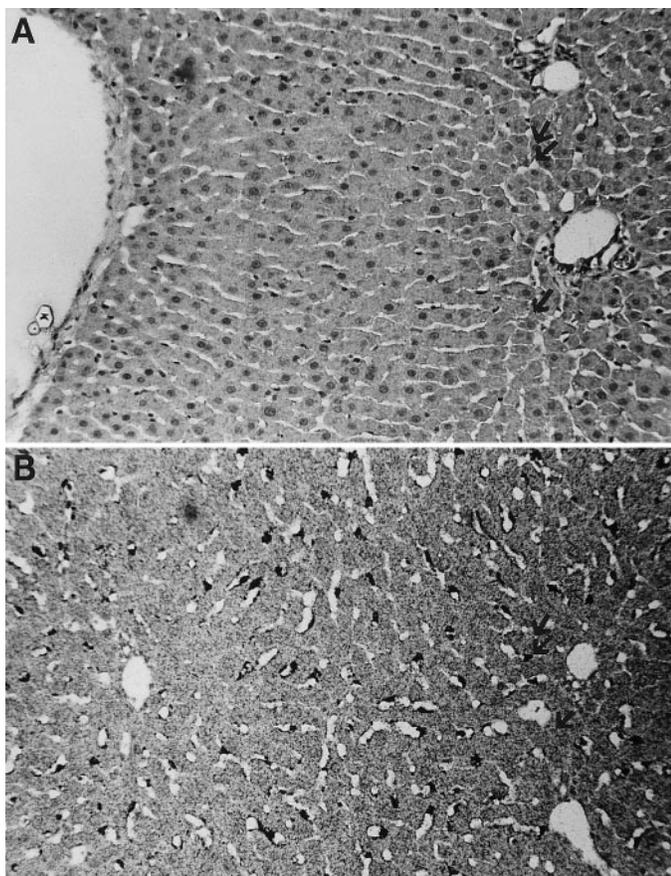
Fig. 6. Autoradiograph of histological liver sections collected from normothermic (*A*) and heat-stressed (*B*) rats, indicating localization of tritium label to hypoxic cells in zones 2 and 3 hepatocytes and Kupffer cells. Hyperthermia did not significantly increase [³H]misonidazole retention in zone 1 cells. Single arrows indicate hepatocytes; double arrows indicate Kupffer cell containing the tritium label.

tion of molecular oxygen, critical considerations during hyperthermia could be hypoxia, cellular acidosis, impaired mitochondrial function, and loss of intracellular ion homeostasis.

[³H]Misonidazole Retention

This project provides the first evidence collected in vivo that heat stress can produce large, regionalized zones of hypoxic cells in the intestinal mucosa and liver. Previous studies that used a variety of methods to experimentally induce hypoxia, including blood vessel clamping (5), administration of 5-hydroxytryptamine (6), and hydralazine (5), have reported increased cellular retention of bioreductive drugs. These studies all had the disadvantage of artificially reducing blood flow, and consequently drug delivery, to the tissues in question. As an alternative to experimentally induced ischemia, we used the hypobaric chamber to physically reduce oxygen partial pressure and have shown that hypobaric hypoxia increases oxygen-dependent retention of [³H]misonidazole (2, 3). Changes in blood flow secondary to hypoxia could not be completely discounted in these studies, but MacManus et al. (30) observed increased misonidazole binding and McAleer

et al. (32) showed increased anti-tumor effects of several bioreductive drugs, suggesting that blood flow was not significantly reduced with this technique. Although an increase in oxygen-independent binding cannot be completely ruled out in the present study, the increased retention of [³H]misonidazole with hyperthermia is comparable to that seen with hypobaric hypoxia that we experimentally induced in rats (2, 3).

In the present experiments, cellular hypoxia was particularly evident in intestinal villi and in small lobules of the liver. Notably, hypoxic label retention was prominent in terminally differentiated cells with high metabolic capacity that are located in regions where the anatomic structure promotes lowered O_2 tensions during periods of ischemia (villus "tip" epithelial cells) (acinus zone 2 hepatocytes). Less metabolically capable cells within the same cell populations (zone 3 hepatocytes, villus epithelial crypt cells) or cells located near blood vessels (zone 1 hepatocytes, villus "base" epithelial cells) retained less [³H]misonidazole. These data are consistent with previous reports that gradients of metabolic activity exist in the small intestine and that ischemia can decrease oxygen delivery to tips of villi due to arteriole-venule O_2 shunting within the villus microvascular network (26, 37). Under ischemic conditions, tips of villi can rapidly become hypoxic, leading to increased permeability to large macromolecules (18). These data are also consistent with reports that O_2 tensions are lower in liver zone 2 and zone 3 hepatocytes during periods of reduced blood flow (34). We have previously shown that heat stress decreases splanchnic blood flow ~50% (27); therefore, the present results suggest that cellular microanatomic location as well as cellular metabolic capacity may be important in determining sensitivity to hyperthermia-induced hypoxic stress. This interpretation is strengthened by previous data from our laboratory suggesting that intestinal and hepatic tissues may be subject to chronic oxidative stress under normal (nonstress) conditions.

We have observed that gradients of immunoreactive antioxidant enzyme and stress protein expression exist within hepatic acini (Hall et al., unpublished observations). In particular, zone 3 hepatocytes show a threefold increase in immunoreactive Cu/Zn superoxide dismutase (SOD), Mn SOD, catalase, and 70-kDa heat shock protein (HSP70) when compared with corresponding cells from zone 1 and an approximately one- to twofold increase over zone 2 cells. Similar results are seen in intestinal villi, where elevated concentrations of immunoreactive Mn SOD, Cu/Zn SOD, catalase, and HSP70 are found in epithelial cells located in the upper third of each villus. Mechanisms responsible for this phenomenon are unknown, but data from the present study would strongly suggest that chronic cellular hypoxic stress may promote ROS generation in these areas, stimulating antioxidant enzyme and stress protein expression. This interpretation is strengthened by the fact that antioxidant enzymes are induced by their respective substrates, and the SODs are specific for O_2^-, whereas catalase is specific for H_2O_2. Interestingly, tips of villi and acinus zone 2 areas are the primary sites of

injury following heat stress, suggesting that these areas may be poised for the cytotoxic effects of hyperthermia. However, further work will be required to determine the involvement of cellular oxidative stress in the pathogenesis of heat-related injury.

Temporary exposure of mammalian cells to hypoxia (22) and heat stress (28) induces a variety of biochemical and physiological changes that can shift cellular redox status toward a prooxidant state, increasing oxypurine flow through purine degradation pathways (12). Under normal conditions, hypoxanthine is metabolized to uric acid by the enzyme xanthine dehydrogenase. Under conditions of hypoxic stress (22) and heat stress (44), this enzyme is rapidly converted to its oxidase form through reversible oxidation of critical sulfhydral groups or after irreversible Ca^{2+}-mediated proteolysis. Because xanthine oxidase can use molecular oxygen as an electron acceptor, it directly produces $O_2^{\cdot-}$ and H_2O_2 as by-products of oxypurine metabolism. Normal or high oxygen tension inhibits xanthine oxidase activity, whereas hypoxia stimulates it, suggesting that O_2 is not a limiting substrate during periods of moderate ischemia (22). Compared with other organs, the rat intestine and liver are rich in xanthine oxidase activity (17, 25), and the pattern of xanthine oxidase expression, high in the duodenum and low in the ileum (25), mirrors the pattern of hyperthermia-related intestinal injury. This is also the case in the liver where hyperthermia-related injury is greatest in areas of high xanthine oxidase expression (44). Moreover, both the liver (44, 48) and the intestine (49) can release xanthine dehydrogenase and xanthine oxidase into the vascular compartment following ischemia. Once exported from the cell, xanthine oxidase can circulate throughout the vascular compartment binding to cell surface glycosaminoglycans at sites distant from its release, producing $O_2^{\cdot-}$ and H_2O_2 adjacent to endothelial and epithelial cell surfaces (48). This type of mechanism is consistent with the widespread tissue injury and organ dysfunction characteristic of hyperthermia. A logical extension of our current results would be to quantitate changes in systemic xanthine oxidase activity and tissue localization of immunoreactive xanthine oxidase protein following heat exposure and heat exposure plus pretreatment with xanthine oxidase antagonists.

Mechanisms responsible for Kupffer cell [^{3}H]misonidazole retention remain obscure, but it is known that, following antigen recognition and phagocytosis, macrophages rapidly increase oxygen consumption in a respiratory burst, generating ROS and hypochlorous acid as part of their antigen killing mechanism (1). Under normothermic conditions, portal venous endotoxin concentration is ~30 ± 7 pg/ml in the rat (21, 36). Heat exposure to a T_c of 41.5°C more than doubles the portal endotoxin concentration (21). Systemic endotoxin levels are unaffected at thermal loads of this magnitude, however, suggesting that the liver clears gut-derived endotoxins under these conditions. These data suggest that Kupffer cell and peritoneal macrophage activation may be increased during heat stress, stimulating increased O_2 consumption and release of acute inflammatory mediators.

This idea is supported by the fact that whole body heat stress increases plasma levels of the inflammatory cytokines tumor necrosis factor-α (TNF-α), interleukin (IL)-1, and IL-6 in humans (10). With the use of a mouse model, Ertel et al. (13) reported that hypoxemia (60-min exposure to 95% N_2-5% O_2) also increases plasma concentrations of TNF-α, IL-1, and IL-6 and markedly elevates cytokine release by peritoneal monocytes and Kupffer cells in vitro, linking mechanisms of hyperthermic and hypoxic cytokine production. Hypoxemia can also stimulate splanchnic release of platelet-activating factor, which in turn elevates inflammatory cytokine release and synergizes with TNF-α in mediating bowel damage (47). In light of our current results, these data would support the hypothesis that hyperthermia stimulates cytokine release through hypoxia-reoxygenation mechanisms or synergizes with hypoxia in initiating an acute inflammatory response that is expanded following mucosal dysfunction and endotoxin translocation into the portal circulation. Clearly, more work is needed to determine the effects of heat stress and intestinal hypoxia on intestinal endotoxin translocation and splanchnic cytokine profile.

In summary, the major findings of this study indicate that arterial-venous O_2 difference is significantly widened in hyperthermic animals both during and after heat exposure, suggesting that intestinal tissues increase oxygen consumption during heat stress. Despite this ability, we have shown for the first time that the concentration of hypoxic cells is increased in the liver and small intestine of hyperthermic animals in vivo. These data support the view that these cells can also be sources of ROS and RNS during heat stress. At this time, it is unclear if the observed cellular hypoxic stress occurs because of decreased oxygen availability, enhanced metabolism, or a combination of these factors, but, like sepsis syndrome, intestinal and hepatic hypoxic stress could be an important early event in the pathogenesis of heat-related illness.

REFERENCES

1. **Babior, B. M.** Oxidants from phagocytes: agents of defense and destruction. *Blood* 64: 959–966, 1984.
2. **Baumgardner, K. R., J. W. Osborne, R. E. Walton, and J. L. Born.** Characterization of induced pulpal hypoxia using ^{3}H-misonidazole. *J. Endod.* 20: 585–588, 1994.
3. **Baumgardner, K. R., R. E. Walton, J. W. Osborne, and J. L. Born.** Induced hypoxia in rat pulp and periapex demonstrated by ^{3}H-misonidazole retention. *J. Dent. Res.* 75: 1753–1760, 1996.
4. **Born, J. L., and B. R. Smith.** The synthesis of tritium-labeled misonidazole. *J. Label. Compounds Radiopharmaceut.* 3: 429–432, 1983.
5. **Bremner, J. C. M., I. J. Stratford, J. Bowler, and G. E. Adams.** Bioreductive drugs and the selective induction of tumor hypoxia. *Br. J. Cancer* 61: 717–721, 1990.
6. **Chaplin, D. J.** Potentiation of RSU-1069 tumor cytotoxicity by 5-hydroxytryptamine (5-HT). *Br. J. Cancer* 54: 727–731, 1986.

7. **Chapman, J. D., A. J. Franko, and J. Sharplin.** A marker for hypoxic cells in tumors with potential clinical applicability. *Br. J. Cancer* 43: 546–550, 1981.

8. **Cobb, L. M., J. Nolar, and P. O'Neill.** Microscopic distribution of misonidazole in mouse tissues. *Br. J. Cancer* 59: 12–16, 1989.

9. **Cobb, L. M., F. R. C. Path, and J. Nolan.** Autoradiographic study of tritium-labelled misonidazole in the mouse. *Int. J. Radiat. Oncol. Biol. Phys.* 16: 953–956, 1989.

10. **D'Oleire, F., C. L. Schmitt, H. I. Robins, J. D. Cohen, and D. Spriggs.** Cytokine induction in humans by 41.8°C whole-body hyperthermia. *J. Natl. Cancer Inst.* 85: 833–834, 1993.

11. **Dykens, J. A.** Isolated cerebral and cerebellar mitochondria produce free radicals when exposed to elevated Ca^{2+} and Na^+: implications for neurodegeneration. *J. Neurochem.* 63: 584–591, 1994.

12. **Elliot, S. J., J. G. Meszaros, and W. P. Schilling.** Effect of oxidant stress on calcium signalling in vascular endothelial cells. *Free Radic. Biol. Med.* 13: 635–650, 1992.

13. **Ertel, W., M. H. Morrison, A. Ayala, and I. H. Chaudry.** Hypoxemia in the absence of blood loss or significant hypotension causes inflammatory cytokine release. *Am. J. Physiol.* 269 (*Regulatory Integrative Comp. Physiol.* 38): R160–R166, 1995.

14. **Franko, A. J.** Misonidazole and other hypoxia markers: metabolism and applications. *J. Rad. Oncol. Biol. Physiol.* 12: 1195–1202, 1986.

15. **Furuyama, F.** Strain differences in thermoregulation of rats surviving extreme heat. *J. Appl. Physiol.* 52: 410–415, 1982.

16. **Gore, I., and N. H. Isaacson.** The pathophysiology of hyperpyrexia. Observations at autopsy in 17 cases of fever therapy. *Am. J. Pathol.* 25: 1029–1060, 1949.

17. **Granger, D. N., M. E. Hollwarth, and D. A. Parks.** Ischemia-reperfusion injury: role of oxygen-derived free radicals. *Acta Physiol. Scand. Suppl.* 548: 47–63, 1986.

18. **Grogaard, B., D. A. Parks, D. N. Granger, J. M. McCord, and O. Forsberg.** Effects of ischemia and oxygen radicals on mucosal albumin clearance in intestine. *Am. J. Physiol.* 242 (*Gastrointest. Liver Physiol.* 5): G448–G454, 1982.

19. **Haglund, U.** Gut ischaemia. *Gut, Suppl.* 1: S73–S76, 1994.

20. **Hall, D. M., G. R. Buettner, R. D. Matthis, and C. V. Gisolfi.** Hyperthermia stimulates nitric oxide formation: electron paramagnetic resonance detection of NO-Heme in blood. *J. Appl. Physiol.* 77: 548–553, 1994.

21. **Hall, D. M., T. D. Oberley, and C. V. Gisolfi.** Hyperthermia increases portal venous endotoxin concentration and upregulates NOS II synthesis (Abstract). *FASEB J.* 11: A121, 1997.

22. **Hasan, N. M., R. B. Cundall, and G. E. Adams.** Effects of hypoxia and reoxygenation on the conversion of xanthine dehydrogenase to oxidase in chinese hamster V79 cells. *Free Radic. Biol. Med.* 11: 179–185, 1991.

23. **Hirst, D. G., J. L. Hazlehurst, and J. M. Brown.** Changes in misonidazole binding with hypoxic fraction in mouse tumors. *Int. J. Radiat. Oncol. Biol. Phys.* 11: 1349–1355, 1985.

24. **Hubbard, R. W., W. D. Bowers, M. T. Matthew, F. C. Curtis, R. E. Criss, G. M. Sheldon, and J. W. Ratteree.** Rat model of acute heatstroke mortality. *J. Appl. Physiol.* 42: 809–816, 1977.

25. **Jarasch, E. D., G. Bruder, and H. W. Heid.** Significance of xanthine oxidase in capillary endothelial cells. *Acta Physiol. Scand. Suppl.* 548: 39–46, 1986.

26. **Kampp, M., O. Lundgren, and N. J. Nilsson.** Extravascular shunting of oxygen in the small intestine of the cat. *Acta Physiol. Scand.* 72: 396–403, 1968.

27. **Kregel, K. C., P. T. Wall, and C. V. Gisolfi.** Peripheral vascular responses to hyperthermia in the rat. *J. Appl. Physiol.* 64: 2582–2588, 1988.

28. **Laszlo, A.** The effects of hyperthermia on mammalian cell structure and function. *Cell Prolif.* 25: 59–87, 1991.

29. **Lee, P. C., B. R. Bochner, and B. N. Ames.** ApppppA, heat-shock stress, and cell oxidation. *Proc. Natl. Acad. Sci. USA* 80: 7496–7500, 1983.

30. **MacManus, M. P., A. P. Maxwell, W. Abrams, and J. M. Bridges.** The effect of hypobaric hypoxia on misonidazole binding in normal and tumor-bearing mice. *Br. J. Cancer* 59: 349–352, 1989.

31. **Malyshev, I. Y., V. D. Manukhina, L. N. Kubrina, and A. F. Vanin.** Nitric oxide is involved in heat-induced HSP70 accumulation. *FEBS Lett.* 370: 159–162, 1995.

32. **McAleer, M. B., S. R. McKeown, M. P. MacManus, T. R. J. Lappin, and J. M. Bridges.** Hypobaric hypoxia: a method for testing bioreductive drugs in vivo. *Int. J. Radiat. Oncol. Biol. Phys.* 23: 551–555, 1992.

33. **McCord, J. M.** Oxygen-derived free radicals in postischemic tissue injury. *N. Engl. J. Med.* 312: 159–163, 1985.

34. **Metzger, H. P., and M. Schywalsky.** Intraorgan differences of blood flow, oxygen supply and glycogen content in the multilobular liver of normal and hemorrhagic rats. *Int. J. Microcirc. Clin. Exp.* 11: 67–83, 1992.

35. **Mirochnitchenko, O., U. Palnitkar, M. Philbert, and M. Inouye.** Thermosensitive phenotype of transgenic mice overproducing human glutathione peroxidases. *Proc. Natl. Acad. Sci. USA* 92: 8120–8124, 1995.

36. **Olofsson, P., G. Nylander, and P. Olsson.** Endotoxin: routes of transport in experimental peritonitis. *Am. J. Surg.* 151: 443–446, 1986.

37. **Park, P. O., and U. Haglund.** Regeneration of small bowel mucosa after intestinal ischemia. *Crit. Care Med.* 20: 135–139, 1992.

38. **Parliament, M. B., L. I. Wiebe, and A. J. Franko.** Nitroimidazole adducts as markers for tissue hypoxia: mechanistic studies in aerobic normal tissues and tumor cells. *Br. J. Cancer* 66: 1103–1108, 1992.

39. **Raleigh, J. A., A. J. Franko, C. J. Koch, and J. L. Born.** Binding of misonidazole to hypoxic cells in monolayer and spheroid culture: evidence that a side-chain label is bound as efficiently as a ring label. *Br. J. Cancer* 51: 229–235, 1985.

40. **Ropp, M., A. M. Courgeon, R. Calvayrac, and M. Best-Belpomme.** The possible role of superoxide ion in the induction of heat-shock and specific proteins in aerobic *Drosophila* cells during return to normoxia after a period of anaerobiosis. *Can. J. Biochem. Cell Biol.* 61: 456–461, 1983.

41. **Ryan, A. J., R. D. Matthes, F. A. Mitros, and C. V. Gisolfi.** Heat stress does not sensitize rats to the toxic effects of bacterial lipopolysaccharide. *Med. Sci. Sports Exerc.* 26: 687–694, 1994.

42. **Shibolet, S., R. Coll, T. Gilat, and E. Sohar.** Heatstroke: its clinical picture and mechanism in 36 cases. *QJM* 144: 525–548, 1967.

43. **Skibba, J. L., R. H. Powers, A. Stadnicka, D. W. Cullinane, U. A. Almagro, and J. H. Kalbfleisch.** Oxidative stress as a precursor to the irreversible hepatocellular injury caused by hyperthermia. *Int. J. Hyperthermia* 7: 749–761, 1991.

44. **Skibba, J. L., R. H. Powers, A. Stadnicka, and J. H. Kalbfleisch.** The effect of hyperthermia on conversion of rat hepatic xanthine dehydrogenase to xanthine oxidase. *Biochem. Pharmacol.* 37: 4592–4595, 1988.

45. **Spitz, D. R., W. C. Dewey, and G. C. Li.** Hydrogen peroxide or heat shock induces resistance to hydrogen peroxide in chinese hamster fibroblasts. *J. Cell. Physiol.* 131: 364–373, 1987.

46. **Spitz, D. R., and G. C. Li.** Heat-induced cytotoxicity in H_2O_2-resistant Chinese hamster fibroblasts. *J. Cell. Physiol.* 142: 256–260, 1990.

47. **Sun, X.-M., and W. Hseuh.** Bowell necrosis induced by tumor necrosis factor is mediated by platelet activating factor. *J. Clin. Invest.* 81: 1328–1331, 1988.

48. **Tan, S., Y. Yokoyama, E. Dickens, T. G. Cash, B. A. Freeman, and D. A. Parks.** Xanthine oxidase activity in the circulation of rats following hemorrhagic shock. *Free Radic. Biol. Med.* 15: 407–414, 1993.

49. **Terada, L. S., J. J. Dormish, P. F. Shanley, J. A. Leff, B. O. Anderson, and J. E. Repine.** Circulating xanthine oxidase mediates lung neutrophil sequestration after intestinal ischemia-reperfusion. *Am. J. Physiol.* 263 (*Lung Cell. Mol. Physiol.* 7): L394–L401, 1992.

50. **Urtasun, R. C., J. D. Chapman, J. A. Raleigh, A. J. Franko, and C. J. Koch.** Binding of ^{3}H-misonidazole to solid human tumors as a measure of tumor toxicity. *Int. J. Oncol. Biol. Physiol.* 12: 1263–1267, 1986.

51. **Varghese, A. J., S. Gulyas, and J. K. Mohindra.** Hypoxic-dependent reduction of 1-(2-nitro-1-imidazoyl)-3-methoxy-2-propanolol by Chinese hamster ovary cells and KHT tumor cells in vitro and in vivo. *Cancer Res.* 36: 3761–3765, 1976.

52. **Weiss, S. J.** Oxygen, ischemia, and inflammation. *Acta Physiol. Scand. Suppl.* 548: 9–37, 1986.